

On the elastic moduli of two-dimensional assemblies of disks: relevance and modeling of fluctuations in particle displacements and rotations

I. Agnolin*, N.P. Kruyt†

*Groupe Matière Condensée et Matériaux, University of Rennes I
Bat.11A, Campus Beaulieu, 35042 Rennes, France

†Department of Mechanical Engineering, University of Twente
P.O. Box 217, 7500 AE Enschede, The Netherlands
n.p.kruyt@utwente.nl, fax +31(0)534893695

Abstract

We determine the elastic moduli of two-dimensional assemblies of disks by computer simulations. The disks interact through elastic contact forces, that oppose the relative displacement at the contact points by means of a normal and a tangential stiffness, both taken constant. Our simulations confirm that the uniform strain assumption results in inaccurate predictions of the elastic moduli, since large fluctuations in particle displacements and rotations occur. We phrase their contribution in terms of the relative displacement they induce at the contact points. We show that the fluctuations that determine the equivalent continuum behavior depend on the average geometry of the assembly. We further separate the contributions from the center displacement and the particle rotation. The fluctuations result in a relaxation of the system, but along the tangential direction the relaxation is generally entirely due to rotations. We consider two theoretical formulations for predicting the elastic moduli that include the fluctuations, namely the “pair-fluctuation” and the “particle-fluctuation” method. They are both based on the equilibrium of a small subassembly, which is considered representative of the average structure. We investigate the

corresponding predictions of the elastic moduli over a range of coordination numbers and of ratios between tangential and normal stiffness. We find a significant improvement with respect to the uniform strain theory. Furthermore, the dependence of the fluctuations on coordination number and ratio of tangential to normal stiffness is qualitatively captured.

Keywords: granular media, equivalent continuum, elastic moduli, fluctuations, DEM simulations

1 Introduction

This study investigates the elastic mechanical properties of dense random isotropic two-dimensional assemblies of disks. Our work is framed in the context of micromechanics, which focuses on the relation between macroscopic behavior and microscopic interactions. At the macroscopic scale, stress and strain are measured, whose relation is determined by the elastic moduli of the equivalent continuum. At the microscale, forces arise between contacting particles that for quasi-static deformations must satisfy the balance of force and moment for all grains.

In the context of elasticity, contact forces oppose the relative displacement between contacting grains by means of a contact stiffness. The work of Poritzky [1] about contacting thin disks reveals for its normal component a dependence on the overlap that rapidly weakens with the confining pressure. We assume for our assemblies the limit case of constant normal stiffness. Since we focus on small displacements, we also consider the tangential stiffness constant [2, 3]. By ignoring all inhomogeneity in the contact stiffness, we specifically focus on the effects of geometric disorder.

Given the geometry of the contact network, the constitutive law for the contact forces determines the macroscopic mechanical properties once the relative displacements at the contact points are known. Many micromechanical studies [4, 5, 6, 7, 8, 9, 10, 11, 12] use the so-called ‘average strain hypothesis’, where the relative displacements reduce to the contribution from the average strain. The resulting prediction of the elastic moduli is inaccurate [13, 14, 15], particularly for the shear modulus, as in general grains undergo additional displacements in order to attain equilibrium. More sophisticated predictions have recently been developed that incorporate such fluctuations, in [16] for three-dimensional systems and in [17] and [18] for two-dimensional

ones. They are based on the idea that even though the deformation is not uniform, its fluctuations are strongly correlated. The study by Koenders [20] suggests that they occur with correlation lengths in the order of a few diameters, which implies that subassemblies of such a size already contain the essential features of the global structure.

The validity of the theoretical predictions in [17] and [18] is investigated here by comparison with the elastic moduli computed by means of Discrete Element Method (*DEM*) simulations. The analysis is performed for various ratios of tangential to normal stiffness and coordination numbers. We consider assemblies with both larger and smaller coordination number than the onset of iso-staticity for disordered frictionless systems. This onset equals 4 in two dimensions and is recurrent in numerical simulations, as dense assemblies are usually obtained by means of an initial frictionless compression. In experiments [19] on hard disks, coordination numbers smaller and larger than 4 are due, in turn, to the presence of friction and of ordered structures. In DEM simulations, disordered assemblies with larger coordination numbers than the onset of isostaticity can be obtained, for example by neglecting in the constitutive law for the contact force the increase in the normal stiffness with the interpenetration or by applying a large pressure. Such systems are mainly of academic interest, particularly in the development of statistical approaches aimed at predicting the evolution of disordered systems. Also in three dimensions the scientific literature concentrates on samples with larger coordination numbers than the frictionless onset of iso-staticity, which equals 6 in that case. However, studies concerned with the issue of numerically reproducing experimental results [22], [23] emphasize that lower ones might be relevant to practical purposes.

The outline of the study is as follows. Firstly, the basic micromechanical quantities of interest are defined in Section 2. Then, a concise description is given in Section 3 of theoretical approaches for predicting the elastic moduli based, in turn, on the average strain assumption and on the inclusion of displacement fluctuations. The performed DEM simulations are described in Section 4. The corresponding results are analyzed in Section 5 and compared to the results the theoretical predictions. The final section is dedicated to discussion of the results.

2 Micromechanics

We consider the contact between disks p and q of radius R^p and R^q , respectively. The contact is identified by the unit vector n_i^{pq} that points outwards from p along the line that joins the centers. The unit vector t_i^{pq} is tangent to the contact (see Figure 1). In components,

$$\begin{aligned}\mathbf{n}^{pq} &= (\cos \theta^{pq}, \sin \theta^{pq}), \\ \mathbf{t}^{pq} &= (-\sin \theta^{pq}, \cos \theta^{pq}),\end{aligned}$$

where θ^{pq} is the *contact orientation*, counted counterclockwise from the horizontal axis. For future reference, we also define the *branch vector* l_i^{pq} , that joins the centre of particle p to that of particle q pointing outwards from p , i.e.

$$l_i^{pq} = (R^p + R^q) n_i^{pq}.$$

As in monodisperse two-dimensional assemblies crystallization occurs, a log-normal distribution for the particle radii is adopted. Contacting particles

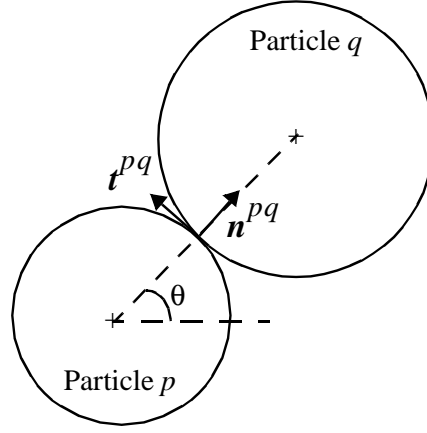


Figure 1: Contact geometry: contact orientation and normal and tangential vectors to the contact.

interact by means of contact forces. We denote by f_i^{pq} the i -th component of the force exerted on particle p by particle q . It has normal and tangential component to the contact f_n^{pq} and f_t^{pq} , i.e.

$$\begin{aligned}f_n^{pq} &= f_i^{pq} n_i^{pq}, \\ f_t^{pq} &= f_i^{pq} t_i^{pq}.\end{aligned}$$

In the hypothesis of quasi-static deformations, contact forces satisfy the balance of force and moment on each grain. For instance, on particle p ,

$$\begin{aligned}\sum_q f_i^{pq} &= 0, \\ \sum_q e_{jk} R^p n_j^{pq} f_k^{pq} &= 0,\end{aligned}$$

where the sum is over particles q that are in contact with it and e_{jk} is the two-dimensional permutation tensor. Contact forces oppose the relative displacement between contacting particles by means of a contact stiffness, whose normal and tangential component we denote, in turn, by k_n and k_t , both considered constant. If we denote by Δ_i^{pq} the relative displacement between particles p and q that are in contact, and by Δ_n^{pq} and Δ_t^{pq} its normal and tangential component, we have

$$\begin{aligned}f_n^{pq} &= k_n \Delta_n^{pq}, \\ f_t^{pq} &= k_t \Delta_t^{pq}, \\ f_i^{pq} &= f_n^{pq} n_i^{pq} + f_t^{pq} t_i^{pq}.\end{aligned}\tag{1}$$

The theory of contact elasticity predicts the decay with the distance from the contact zone of the effects of contact interactions. For small enough deformations and stiff enough particles, as we assume to be the case here, contact interactions can be assumed to be confined to a contact point, and the grains kinematics to be approximated by that of rigid bodies. Therefore,

$$\Delta_i^{pq} = U_i^q - U_i^p + e_{ij} (R^q \Omega^q + R^p \Omega^p) n_i^{pq},$$

where U_i^p and U_i^q are the displacement of the centre of particle p and q , Ω^p and Ω^q their rotation.

At the macroscopic, continuum level, the relevant quantities are the stress tensor σ_{ij} and the strain tensor ϵ_{ij} , whose components are taken positive in compression. Contact forces and the geometry of the particle arrangement determine the expression of the former, as [24, 25, 26]

$$\sigma_{ij} = \frac{1}{S} \sum_{\theta_g} \sum_{c \in C(\theta_g)} f_i^c t_j^c,\tag{2}$$

that is the average over the area of interest S of Cauchy's stress [27]. The orientation θ_g varies between 0 and π . Finally, the superscript pq referring

to contacting particles has been replaced by for corresponding contacts c . Expression (2) emphasizes the dependence of the macroscopic behavior on the average force over equally oriented contacts. Experimental observations and numerical simulations [28, 29, 30] suggest for it the same dependence on the contact orientation as for the effects of the average strain. That is, compressive forces are the larger the closer the contact orientation is to the direction of major compression, and tangential forces have their maximum at contacts oriented at 45 degrees from it.

Primary geometrical characteristics of granular assemblies are coordination number Γ , i.e. the average number of contacts per particle, contact density n_S , i.e. the average number of particles per unit surface, and the contact distribution function $E(\theta)$ [31], defined such that $E(\theta)d\theta$ gives the probability of finding a contact with orientation θ in the interval $(\theta, \theta + d\theta)$, $\theta \in (0, \pi)$. In the case of *isotropic* assemblies, as considered here, the contact distribution function becomes $E(\theta) = 1/\pi$. With the use of such quantities and by denoting averages over equally oriented contacts by overbars, expression (2) transforms into the integral

$$\sigma_{ij} = \frac{n_S \Gamma}{2} \int_0^\pi E(\theta) \overline{f_i l_j}(\theta) d\theta. \quad (3)$$

The elastic stiffness tensor relates stress and strain. In isotropic systems, it is fully described by the effective bulk modulus K and shear modulus G , as

$$\begin{aligned} \sigma_{11} + \sigma_{22} &= 2K(\epsilon_{11} + \epsilon_{22}) \\ \sigma_{11} - \sigma_{22} &= 2G(\epsilon_{11} - \epsilon_{22}). \end{aligned} \quad (4)$$

We determine them by means of DEM computer simulations, by applying, in order, an isotropic compressive deformation ϵ_{ij}^K and a shear deformation ϵ_{ij}^G :

$$\epsilon_{ij}^K = \epsilon_0 \begin{pmatrix} 1 & 0 \\ 0 & 1 \end{pmatrix}, \quad \epsilon_{ij}^G = \epsilon_0 \begin{pmatrix} 1 & 0 \\ 0 & -1 \end{pmatrix}, \quad (5)$$

and measuring the corresponding stress response. By ϵ_0 we denote a magnitude of the imposed strain.

3 Theoretical modeling

If the deformation ϵ_{ij} is prescribed, the theoretical prediction of the elastic moduli requires that of the corresponding stress tensor σ_{ij} . Due to (1), this

in turn requires a kinematic localization assumption, that is, the expression of the relative displacements between contacting particles as a function of ϵ_{ij} . This procedure is depicted in Figure 2. Various kinematic localization assumptions are considered in this section, such as the uniform strain assumption and more sophisticated approaches that account for fluctuations.

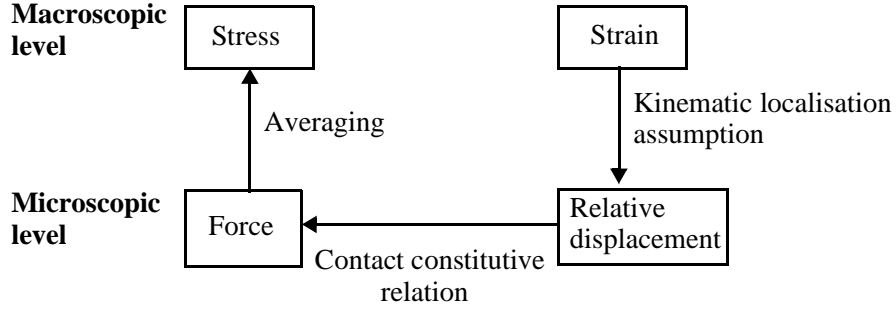


Figure 2: Kinematic localisation assumption.

3.1 Uniform strain

In the hypothesis of uniform strain the relative displacement between contacting particles becomes

$$\Delta_i^{pq} = \epsilon_{ij} l_j^{pq}.$$

Its average over equally oriented contacts in the case of isotropic compression is isotropic. Only its normal component $\Delta_n^{\epsilon, is}$ differs from zero, namely

$$\Delta_n^\epsilon = \epsilon_0 \bar{l}, \quad (6)$$

where \bar{l} is the average length of the branch vector. In the case of shear, the average normal and tangential component Δ_n^ϵ and Δ_t^ϵ of Δ_i^{pq} over equally oriented contacts are, in turn,

$$\begin{aligned} \Delta_n^\epsilon(\theta) &= \epsilon_0 \bar{l} \cos 2\theta, \\ \Delta_t^\epsilon(\theta) &= -\epsilon_0 \bar{l} \sin 2\theta. \end{aligned} \quad (7)$$

For isotropic assemblies of disks, the average strain assumption results in the bulk and shear moduli K^ϵ and G^ϵ [8]:

$$\begin{aligned}\frac{K^\epsilon}{k_n} &= \frac{n_s \Gamma}{8} \overline{l^2} \\ \frac{G^\epsilon}{k_n} &= \frac{n_s \Gamma}{16} \left[1 + \frac{k_t}{k_n} \right] \overline{l^2},\end{aligned}\tag{8}$$

that are upper bounds. The symbol $\overline{l^2}$ denotes the average over all contacts of the squared length of the branch vector. As discussed in [32], polydispersity makes the average length of the branch vector differ in general from the average diameter. For our size distribution \bar{l} is about 3% larger than the average diameter, and $\overline{l^2}$ is about 15% larger than the average diameter squared.

3.2 Approaches that incorporate displacement fluctuations

Two approaches are considered that incorporate the fluctuations into the prediction of the elastic moduli, namely the particle-fluctuation (1PF) and the pair-fluctuation method (PF). They are discussed in detail in [17] and in [18], respectively. In [17], the 1PF approach is applied numerically and proven to give upper bounds to the effective moduli, while in [18] the analytical solution that corresponds to the PF method is presented. Both approaches deal with the issue of equilibrium of a small assembly, made of a chosen particle A and of a contacting pair AB , respectively, surrounded by their first neighbors. Therefore, in these models fluctuations are assumed to occur with correlation lengths in the order of 3 or 4 diameters.

In the more general case, the relative displacement between contacting particles can be decomposed into the contribution from averages and fluctuations, that is, from the imposed strain and the average particle rotation, on one side, and from fluctuations in particle displacements and rotations, on the other. In the absence of macroscopic rotation, as it is the case here, in an isotropic system the average particle rotation is zero [33]. If we denote by \tilde{u}_i^p and \tilde{u}_i^q the fluctuation of contacting particles p and q in the center displacement, and by $\tilde{\omega}^p$ and $\tilde{\omega}^q$ the fluctuations in rotations, we can write:

$$\Delta_i^{pq} = \epsilon_{ij} l_j^{pq} + (\tilde{u}_i^q - \tilde{u}_i^p) - (R^q \tilde{\omega}^q + R^p \tilde{\omega}^p) t_i^{pq}.$$

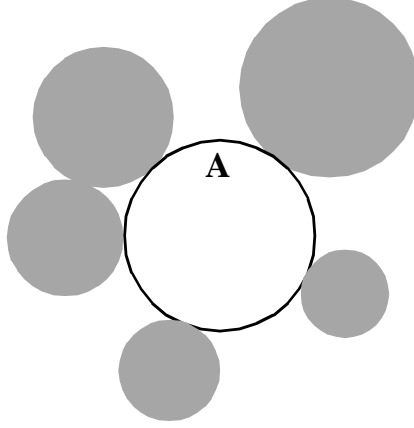


Figure 3: Small assembly considered in the "particle-fluctuation" method, centered on particle A . The deformation of the particles shown in gray is according to uniform strain, while A is allowed to fluctuate. Its fluctuations stem from the balance of force and moment on it.

In the 1PF and the PF approach, only the chosen particle or pair is allowed to fluctuate, while their neighborhood is compelled to move according to the average strain. This is depicted in Figure 3 for the 1PF case. As a result, in the 1PF method the relative displacement between particle A and its r -th neighbor reduces to

$$\Delta_i^{Ar} = \epsilon_{ij} l_j^{Ar} - \tilde{u}_i^A - R^A \tilde{\omega}^A t_i^{Ar},$$

so that the three equilibrium equations for particle A can be solved for its three unknown fluctuations. In the pair-fluctuation method,

$$\Delta_i^{AB} = \epsilon_{ij} l_j^{AB} + (\tilde{u}_i^B - \tilde{u}_i^A) - (R^A \tilde{\omega}^A + R^B \tilde{\omega}^B) t_i^{AB},$$

but

$$\begin{aligned} \Delta_i^{Ar} &= \epsilon_{ij} l_j^{Ar} - \tilde{u}_i^A - R^A \tilde{\omega}^A t_i^{Ar}, \\ \Delta_i^{Bs} &= \epsilon_{ij} l_j^{Bs} - \tilde{u}_i^B - R^B \tilde{\omega}^B t_i^{Bs}, \end{aligned}$$

where r denotes a neighbor of particle A different from B , and s a neighbor of particle B different from A . The six equilibrium equations of particles A

and B can be solved for the corresponding six fluctuations. In both cases, the small size of the solving system permits an analytical formulation.

In this work, the equilibrium equations are solved numerically, particle by particle and pair by pair for the 1PF and the PF approach, respectively, for the corresponding fluctuations. Using the procedure sketched in Figure 2, the corresponding contact forces are computed and the stress and elastic moduli estimated. The resulting fluctuations are also analyzed in terms of the associated deformation mechanisms in the sections that follow.

4 DEM simulations

DEM simulations have been performed of large isotropic assemblies of 50,000 disks, with radii from a lognormal distribution. Periodic boundaries have been employed to reduce boundary effects.

In the DEM method, the deformation of the assemblies is computed by numerically integrating in time the equations of motion of all particles, and the results can be employed to analyze the actual deformation mechanisms.

Initial equilibrium states with coordination numbers $\Gamma = 3.5$, $\Gamma = 4$ and $\Gamma = 5$ have been first prepared. To obtain the first one, a succession of frictionless and frictional compressions has been employed. The second one results from the isotropic compression of a frictionless gas, and the third one results from an additional isotropic compression.

The assemblies obtained this way have been subjected to the two strain paths specified by eqn.(5). Then, the corresponding stress response has been computed in order to determine the effective bulk and shear moduli K and G . Such simulations have been performed with bonded contacts: that is, neither contact creation nor disruption has been considered, which is appropriate for studying elastic behavior at small strains. At each coordination number, different ratios k_t/k_n have been used, in the range between 0.05 and 1.0.

5 Micromechanical analysis

In this section, the results from the DEM simulations and the theoretical approaches introduced in Section 3 are analyzed. The comparison between the elastic moduli from the DEM simulations and the uniform strain assumption emphasizes the relevance of displacement fluctuations. The quality of the

estimates of the elastic moduli given by the 1PF and the PF methods is also evaluated. Then, the deformation mechanisms induced by the fluctuations at the macroscopic scale are analyzed, and the performance of the 1PF and PF approaches interpreted in terms of their capability of capturing them.

5.1 Moduli

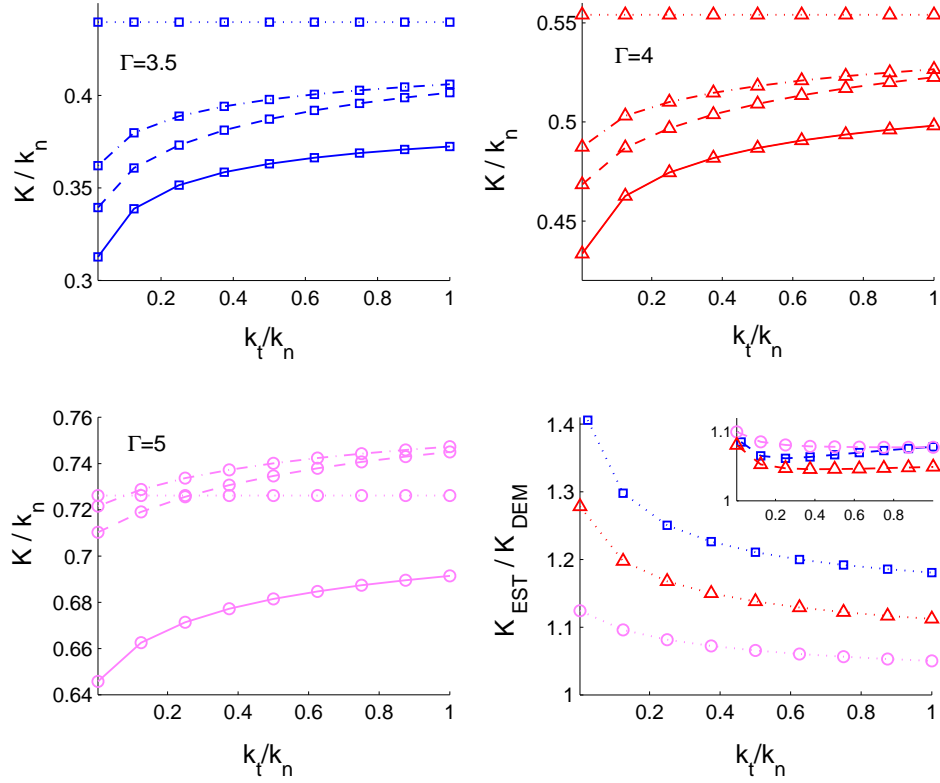


Figure 4: Bulk modulus K : from DEM simulations (solid line), uniform strain assumption (dotted line), 1PF (dashed) and PF (dashed-dotted) approaches. Results for three coordination numbers Γ : $\Gamma = 3.5$ (\square), $\Gamma = 4$ (\triangle), $\Gamma = 5$ (\circ) and various stiffness ratios k_t/k_n . Bottom right: estimate performance for uniform strain assumption (dotted) and 1PF approach (dashed), for $\Gamma = 3.5, 4.0, 5.0$.

The bulk and shear moduli that result from the DEM simulations and the theoretical approaches discussed in Section 3 are compared in Figures

4 and 5. They are presented in the dimensionless form K/k_n and G/k_n , as function of the ratio k_t/k_n and for the three chosen coordination numbers. In the fourth frame of the two figures, the quality of the estimates is plotted in terms of their ratio to the effective moduli. The average strain prediction

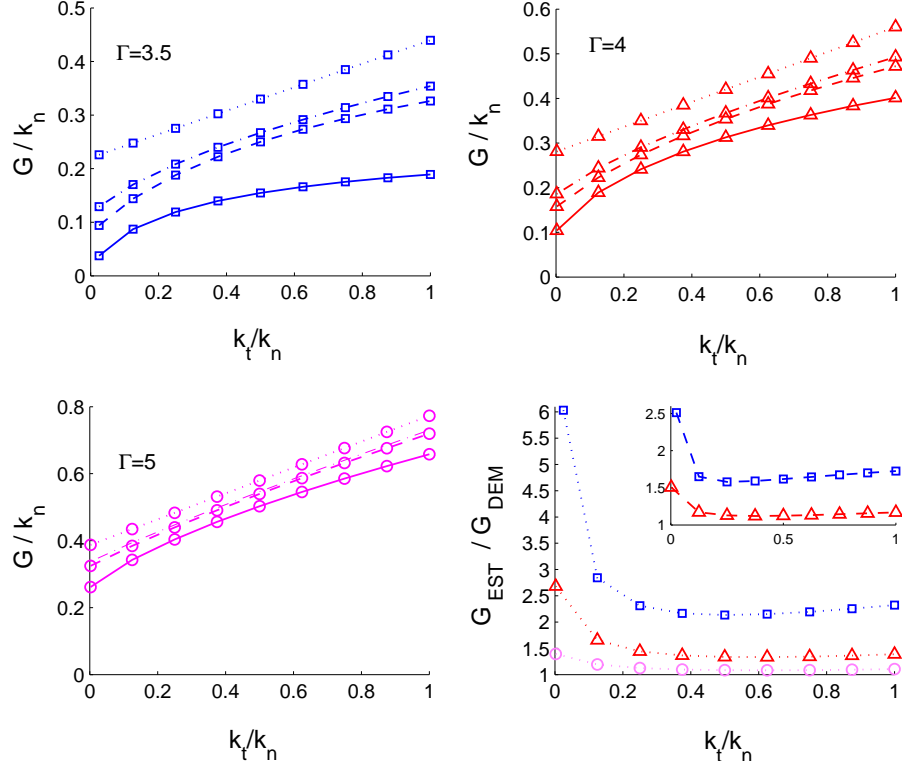


Figure 5: Shear modulus G . Same symbols as in Figure 4.

performs poorly, especially at small coordination numbers. The inclusion of the fluctuations with as few degrees of freedom as in the 1PF and PF methods does not guarantee an improvement with respect to the average strain assumption, as the case of the bulk modulus at $\Gamma = 5$ proves.

The DEM simulations point out the dependence of the bulk modulus on the tangential stiffness, ignored by the average strain assumption, but captured once fluctuations are accounted for. The reason for such a dependence lies in the fact that even though the tangential forces are zero on average in hydrostatic compression, they are required at the particle level in order for the forces and moments to balance. By opposing the relative

displacements along the tangential direction, the tangential forces stiffen the assembly, the more so the larger the tangential stiffness. The general belief that the average strain assumption gives a good approximation of the bulk modulus seems hardly acceptable, at least below the onset of iso-staticity for frictionless systems and at small ratios k_t/k_n . Regarding the shear modulus, the inclusion of the fluctuations into the prediction results in a significant improvement with respect to the average strain assumption, although important deviations from the DEM simulations remain, especially for low coordination number and low stiffness ratios k_t/k_n .

5.2 Relative displacements

At the macroscopic level, only the average over equally oriented contacts of the relative displacement between contacting particles is important, as follows from (1) and (2). We label by $\tilde{\Delta}_i^{pq}$ the relative displacement between contacting grains p and q due to their fluctuations:

$$\tilde{\Delta}_i^{pq} \doteq \tilde{u}_i^q - \tilde{u}_i^p - (R^p \tilde{\omega}^p + R^q \tilde{\omega}^q) t_i^{pq},$$

and by $\tilde{\Delta}_n^{pq}$ and $\tilde{\Delta}_t^{pq}$ its normal and tangential component,

$$\begin{aligned} \tilde{\Delta}_n^{pq} &= (\tilde{u}_j^q - \tilde{u}_j^p) n_j^{pq} \\ \tilde{\Delta}_t^{pq} &= (\tilde{u}_j^q - \tilde{u}_j^p) t_j^{pq} - (R^q \tilde{\omega}^p + R^p \tilde{\omega}^q). \end{aligned}$$

When an isotropic compression is applied, only the former contributes to the stress. Its distribution is uniform and has average $\overline{\tilde{\Delta}_n}$, such that

$$\overline{\tilde{\Delta}_n} = \beta_n \Delta_n^\epsilon, \quad (9)$$

where Δ_n^ϵ is given by expression (6). As the fluctuations relax the system, β_n is negative. It follows after some algebra from (2), the first of (8) and (9) that

$$K = (1 + \beta_n) K^\epsilon. \quad (10)$$

Corresponding values of K^ϵ/K are shown in the fourth frame of Figure (4).

Typical group averages for the case of shear loading are shown in Figure 6, where along the tangential direction the contributions from the center displacement and the rotation have been separated. The average normal and tangential relative displacements induced by the fluctuations over equally

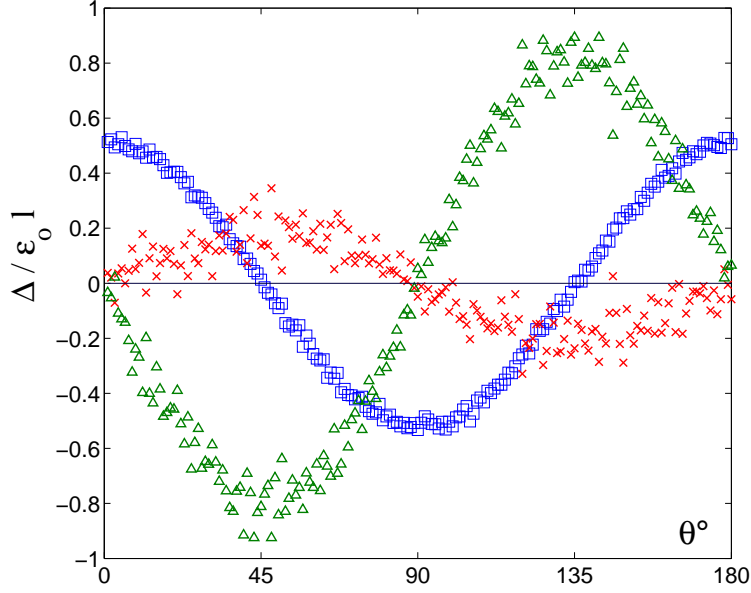


Figure 6: Relative displacements between contacting particles averaged over equally oriented contacts: normal component (\square), tangential component due to center displacements (\triangle) and rotations (\times). Results for shear deformation at coordination number $\Gamma = 3.5$ and stiffness ratio $k_t/k_n = 0.5$.

oriented contacts are proportional to those of eqn.(7), induced by the average strain and aligned with them. Hence we can write [32]:

$$\begin{aligned}\overline{\Delta}_n(\theta) &= \alpha_n \Delta_n^\epsilon(\theta) \\ \overline{\Delta}_t(\theta) &= \alpha_t \Delta_t^\epsilon(\theta).\end{aligned}$$

The contributions from the particle displacements and rotations to $\overline{\Delta}_t$ are characterized by analogous coefficients α_t^u and α_t^ω , such that

$$\alpha_t = \alpha_t^u + \alpha_t^\omega.$$

Considerations analogous to those arisen from expression (??) allow one to write the effective shear modulus as

$$\frac{G}{k_n} = (1 + \alpha_n) \left[1 + \frac{(1 + \alpha_t)k_t}{(1 + \alpha_n)k_n} \right] \frac{n_S \Gamma}{16} \overline{l^2}.$$

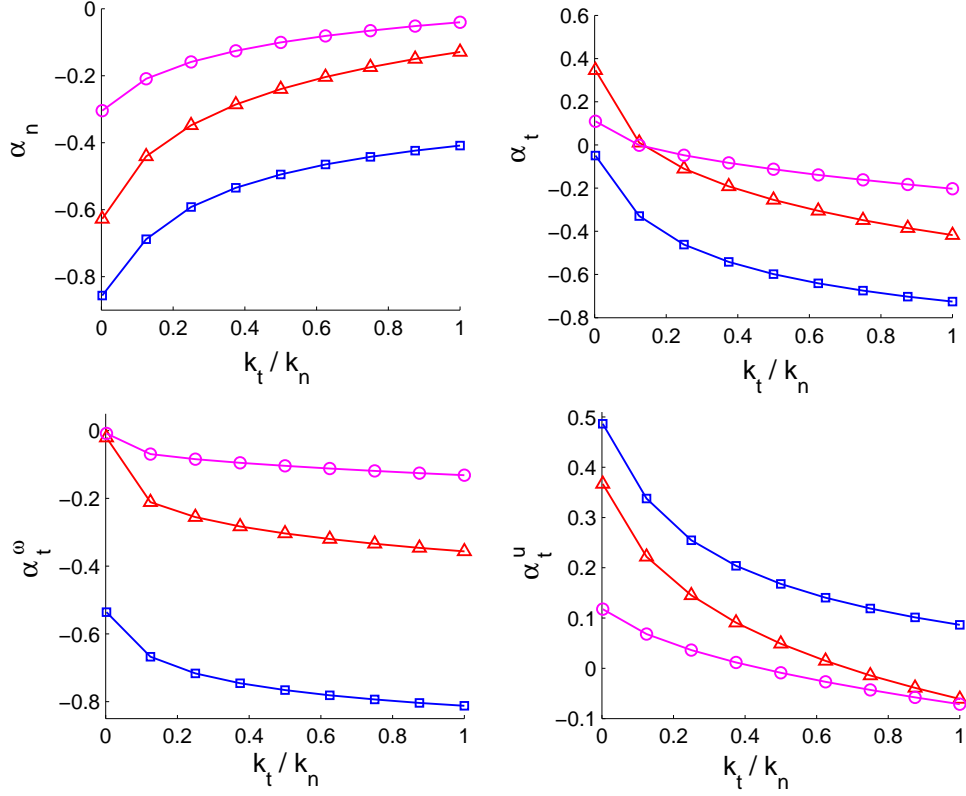


Figure 7: Magnitude of fluctuations in the relative displacements in terms of α_n^{sh} , α_t , α_t^ω and α_t^u . Results from DEM simulations for three coordination numbers Γ : $\Gamma = 3.5$ (\square), $\Gamma = 4$ (\triangle), $\Gamma = 5$ (\circ) and various stiffness ratios k_t/k_n .

5.3 Magnitude of observed and predicted fluctuations

In the case of isotropic compression, Figure 4 shows that the prediction of β_n is satisfactory.

As regards shear, the dependence of α_n , α_t , α_t^u and α_t^ω on coordination number and stiffness ratio k_t/k_n is shown in Figure 7. Negative numerical factors mean a relaxation with respect to the average strain assumption. The magnitude of the fluctuations decreases with increasing coordination number and, as expected, is more important when the system is undergoing shear deformation. Both the normal and the tangential component of the fluctuations relax the system with respect to the average strain assumption,

but along the tangential direction the relaxation is almost exclusively due to the particle rotation. On the contrary, the center displacements generally induce average relative displacements of the same sign as those due to the average strain. The predictions that include the fluctuations result in group-

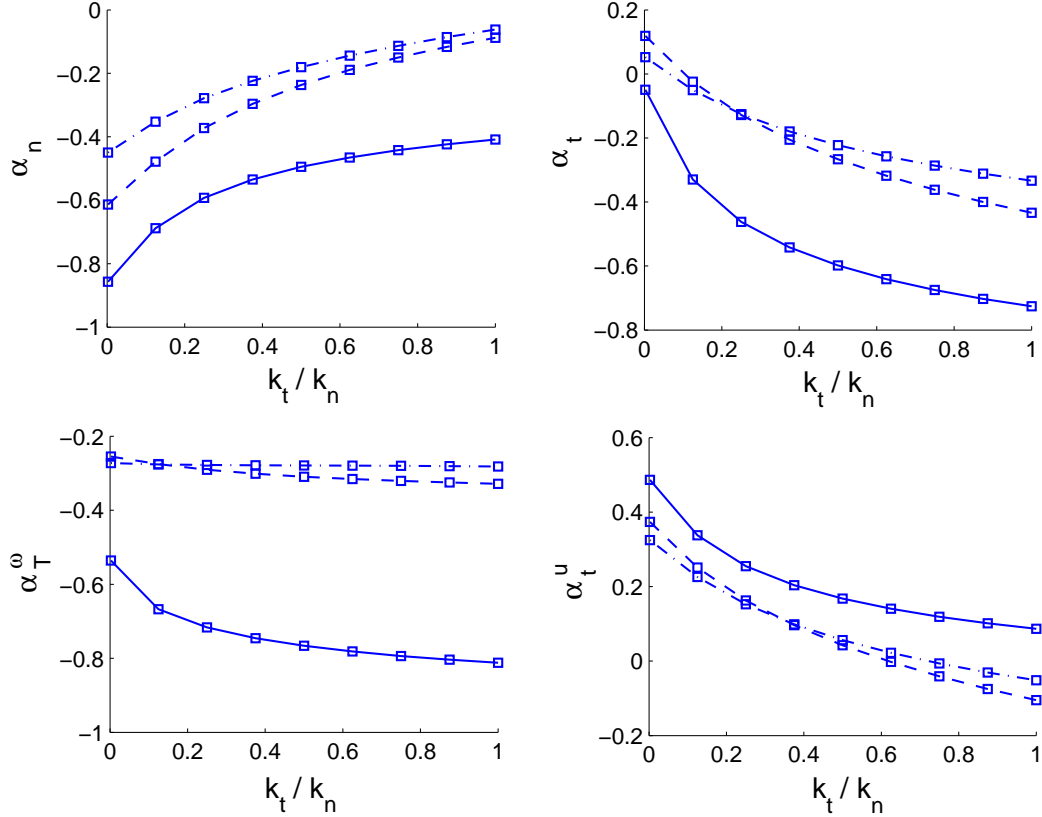


Figure 8: Comparison between α_n , α_t , α_t^u and α_t^ω from DEM simulation (solid line), 1PF (dashed) and PF-theory (dashed-dotted). Results for $\Gamma = 3.5$ and various stiffness ratios k_t/k_n .

averages analogous to those of Figure 7. The corresponding factors α_n , α_t , α_t^u and α_t^ω are plotted in Figure 8 for coordination number $\Gamma = 3.5$. Their trend stays unchanged for the other coordination numbers considered. The estimates qualitatively reproduce the observed dependence of the fluctuations on k_t/k_n and on coordination number Γ . However, the relaxation they induce is underestimated, and the stiffening observed in the case of the particle displacement generally overestimated. The difference between estimate and

measured values at low coordination number in the case of shear emphasizes the necessity of considering larger correlation lengths if reliable predictions of the mechanical behavior of such systems are to be obtained. Given the remarkable improvement already obtained with respect to the average strain assumption, it might be sufficient to incorporate the fluctuations of the first neighbors.

6 Discussion and perspectives

This study has emphasized the insufficiency of the average strain assumption in predicting the elastic moduli of granular media, especially in presence of shear, as particles undergo important additional displacements and rotations in order to attain equilibrium. This particularly holds in the case of coordination numbers smaller than that corresponding to the onset of iso-staticity for frictionless assemblies, whose occurrence seems relevant to practical purposes.

We have shown that the role of the fluctuations is clearly phrased in terms of the relative displacements they induce at the contact points, coherently with the constitutive law for the contact forces. The relative displacements due to the fluctuations are highly correlated with contact orientation. Along the normal and the tangential direction, respectively, their average over equally oriented contacts is proportional to the relative displacements aligned with them and due to the average strain. Such a proportionality is expressed by the numerical factors β_n for the case of isotropic compression, and α_n , α_t^u and α_t^ω in the case of shear. Their numerical value allows one to interpret the role of the different kinematic ingredients to the relaxation observed at the macroscopic scale. We have found that the normal component of the center displacements and the rotations always oppose the effect of the average strain. On the contrary, the tangential component of the center displacements generally stiffens the assembly, with the exception of large ratios k_t/k_n at large coordination number.

We have analyzed two approaches that include the fluctuations from the average strain into the prediction of the elastic moduli, namely the "particle-fluctuation" and the "pair-fluctuation" method. They both determine the fluctuations by considering the problem of equilibrium of a small subassembly. That is, they are based on the assumption that the fluctuations organize with short correlation length, in the order of three or four diameters. The

comparison with the DEM simulations shows a significant improvement in predicting the moduli with respect to the average strain assumption. The deformation mechanisms are qualitatively captured, even at small coordination numbers, together with their dependence on the ratio between tangential and normal stiffness and on coordination number, thus proving the correctness of the approach. However, the models do not capture with sufficient accuracy the fluctuations at low coordination numbers when a shear loading is applied (especially for the tangential relative displacements). This may be caused by the occurrence of larger correlation lengths than those assumed here.

Future work will focus on identifying the correct correlation length. An other open issue is the mechanical behavior at ratios of tangential to normal stiffness larger than one, that easily occur at the contact between cylinders far from the onset of sliding. The independence of the α 's on the contact orientation assesses that the fluctuations that determine the macroscopic behavior originate in the average geometry of the assembly. Therefore, analytical approaches can capture them. As the average geometry is disordered, its representation has to be resolved in statistical terms, as done in the analytical solution in [18]. Even though the issue has not been dealt with in this manuscript, we anticipate that the cited analytical prediction gives less accurate results than the numerical implementation of the corresponding approach. This emphasizes the sensitivity of the modeling to the details of the statistical representation. This representation is still a critical issue whose improvement we will pursue.

7 Acknowledgments

The authors acknowledge financial support of the first author, during her stay at the University of Twente, by IMPACT, the research institute of the University of Twente on Mechanics, Processes and Control. Financial support has also been given by "Gruppo Nazionale di Fisica Matematica" of the "Istituto Nazionale di Alta Matematica" through the Research Project "Constitutive Models for Granular Materials".

References

- [1] Poritsky, H. (1950). Stresses and deflections of cylindrical bodies in contact with application to contact of gears and of locomotive wheels, *Journal of Applied Mechanics* 17: 191-201.
- [2] Mindlin, R.D., Deresiewicz, H. (1953). Elastic spheres in contact under varying oblique forces, *Journal of Applied Mechanics* 20: 327-344.
- [3] Johnson, K.L. (1985). *Contact Mechanics*. Cambridge University Press, Cambridge.
- [4] Rothenburg, L. 1980. Micromechanics of idealised granular materials. PhD Thesis Department of Civil Engineering, Carleton University, Ottawa, Ontario, Canada.
- [5] Digby, P.J. (1981). The effective moduli of porous granular rock. *Journal of Applied Mechanics* 48: 803-808.
- [6] Christoffersen, J., Mehrabadi, M.M., Nemat-Nasser, S. (1981). A micro-mechanical description of granular material behaviour, *Journal of Applied Mechanics* 48: 339-344.
- [7] Walton, K. (1987). The effective elastic moduli of a random packing of spheres, *Journal of the Mechanics and Physics of Solids* 35: 213-226.
- [8] Bathurst, R.J., Rothenburg, L. (1988a). Micromechanical aspects of isotropic granular assemblies with linear contact interactions. *Journal of Applied Mechanics (Transactions of the ASME)* 55: 17-23.
- [9] Bathurst, R.J., Rothenburg, L. (1988b). Note on a random isotropic granular material with negative Poisson's ratio. *International Journal of Engineering Science* 26: 373-383.
- [10] Chang, C.S., Misra, A., Sundaram, S.S. (1990). Micro-mechanical modelling of cemented sands under low amplitude oscillations. *Géotechnique* 40: 251-263.
- [11] Chang, C.S., Chao, S.J., Chang, Y. (1995). Estimates of elastic moduli for granular material with anisotropic random packing structure. *International Journal of Solids and Structures* 32: 1989-2008.

- [12] Cambou, B., Dubujet, P., Emeriault, F., Sidoroff, F. (1995). Homogenisation for granular materials. *European Journal of Mechanics A / Solids* 14: 255-276.
- [13] Makse, H.A., Gland, N., Johnson, D.L., Schwartz, L.M. (1999). Why effective medium theory fails in granular materials. *Physical Review Letters* 83: 5070-5073.
- [14] Rothenburg, L., Kruyt, N.P. (2001). On limitations of the uniform strain assumption in micromechanics of granular materials. *Powders and Grains 2001*, pp.191-194, ed. Y. Kishino, Balkema Publishers, Rotterdam, The Netherlands.
- [15] Suiker, A.S.J., Fleck, N.A. (2004). Frictional collapse of granular materials. *Journal of Applied Mechanics* 71: 350-358.
- [16] Jenkins, J.T., Johnson, D., La Ragione, L., Makse, H. (2005). Fluctuations and the effective moduli of an isotropic, random aggregate of identical, frictionless spheres. *Journal of the Mechanics and Physics of Solids* 53: 197-225
- [17] Kruyt, N.P., Rothenburg, L. (2004). Kinematic and static assumptions for homogenization in micromechanics of granular materials. *Mechanics of Materials* 36: 1157-1173.
- [18] Agnolin, I., Jenkins, J.T., La Ragione L. (2005). A continuum theory for a random array of identical, elastic, frictional disks. *Mechanics of Materials*, accepted for publication (available on line).
- [19] Gervois, A., Bideau D. (1992). Some geometrical properties of two-dimensional hard disks packings. *Disorder and granular media*, Ed. Bideau and Hansen, North-Holland, 1-31.
- [20] Gaspars, N., Koenders, M.A. (2001). Micromechanical formulation of macroscopic structures in a granular medium. *Journal of Engineering Mechanics* 127: 987-992.
- [21] Cundall, P.A., Strack, O.D.L. (1979). A discrete numerical model for granular assemblies. *Géotechnique* 9: 47-65.

- [22] Cundall, P.A., Jenkins, J.T., Ishibashi, I. (1989). Evolution of elastic moduli in a deforming granular assembly. *Powders and Grains 1989*, Ed. J. Biarez, R. Gouvres.
- [23] Agnolin, I., Roux, J.N. Elastic moduli of numerical assemblies of spheres: the role of the fluctuations from the average strain. In preparation.
- [24] Drescher, A., de Josselin de Jong, G. (1972). Photoelastic verification of a mechanical model for the flow of a granular material. *Journal of the Mechanics and Physics of Solids* 20 337-351.
- [25] Strack, O.D.L., Cundall, P.A. (1978). The distinct element method as a tool for research in granular media: part I. Report National Science Foundation, NSF Grant ENG75-20711.
- [26] Rothenburg, L., Selvadurai, A.P.S. (1981). A micromechanical definition of the Cauchy stress for particulate media. In: *Proceedings International Symposium on Mechanical Behaviour of Structured Media*, pp. 469-486, ed. A.P.S. Selvadurai, Ottawa, Canada.
- [27] Love, A.E.H. (1944). *A treatise on the mathematical theory of elasticity*. Dover Publications, New York.
- [28] Bathurst, R.J., Rothenburg, L. (1990). Observations on stress-force-fabric relationships in idealized granular materials. *Mechanics of Materials* 9: 65-80.
- [29] Calvetti, F., Emeriault, F. (1999). Interparticle force distribution in granular materials: link with the macroscopic behavior. *Mechanics of Cohesive-Frictional Materials* 4: 247-279.
- [30] Rothenburg, L., Bathurst, R.J. (1989). Analytical study of induced anisotropy in idealized granular materials. *Geotechnique* 39: 601-614.
- [31] Horne, M.R. (1965). The behaviour of an assembly of rotound, rigid, cohesionless particles I and II. *Proceedings of the Royal Society London A* 286: 62-97.
- [32] Kruyt, N.P., Rothenburg, L. (2001). Statistics of the elastic behaviour of granular materials. *International Journal of Solids and Structures* 38: 4879-4899.

- [33] Jenkins, J.T., La Ragione, L. (1999). Particle spin in anisotropic granular materials. *International Journal of Solids and Structures* 38: 1063-1069.
- [34] Kruyt, N.P., Rothenburg, L. (2002). Micromechanical bounds for the elastic moduli of granular materials. *International Journal of Solids and Structures* 39: 311-324.
- [35] Agnolin, I., Roux, J.N. (2005). Elasticity of sphere packings: pressure and initial state dependence. *Powders & Grains 2005*, pp.87-91, eds. R. Garcia-Rojo, H.J. Hermann, S. McNamara, Balkema Publishers, Rotterdam, The Netherlands.